Journal of Pharmaceutical, Chemical and Biological Sciences
ISSN: 2348-7658
Impact Factor (GIF): 0.615
Impact Factor (SJIF): 2.092
June-August 2015; 3(2):247-261
Available online at http://www.jpcbs.info

Original Research Article

Alleviation of Doxorubicin-Induced Cardiocytotoxicity by Anthocyanin-Rich Bilberry (Vaccinium myrtillus L.) in H9c2 Cells by Antioxidative Effects

Eun Hye Choi[1,2], Jin-Yi Han[1], Ju Hee Kang[1], Mi Kyung Kim[2], Hyang Sook Chun[1]*

[1]School of Food Science and Technology, Chung-Ang University, Ansung, Gyounggi 456-756, Republic of Korea
[2]Department of Food & Nutritional Sciences, Ewha Womans University, 11-1 Daehyun-dong, Seodaemun-gu, Seoul, Republic of Korea
(Eun Hye Choi and Jin-Yi Han equally contributed to this work)

***Corresponding Author:** Dr. Hyang Sook Chun, Department of Food Science and Technology, Chung-Ang University, Naeri 72-1, Ansung, Kyonggi 456-756, Republic of Korea

Received: 24 July 2015 Revised: 31 July 2015 Accepted: 03 August 2015

ABSTRACT

To evaluate the protective effects of anthocyanin-rich bilberry extract (BE) against doxorubicin (Dox)-induced cytotoxicity, this study examined cytotoxicity, apoptosis, mitochondria dysfunction and cellular redox status in H9c2 cells. Dox exposure significantly induced cytotoxicity, DNA fragmentation and caspase-3 activity, mitochondrial dysfunction, intracellular reactive oxygen species (ROS) generation and lipid peroxidation in H9c2 cells. The addition of BE to H9c2 cells significantly reduced intracellular ROS generation, glutathione (GSH) levels and restored mitochondrial transmembrane potential (MTP), inhibited caspase-3 activity, activated glutathione S-transferases (GSTs) and finally, reduced apoptosis and cell death. Furthermore, cDNA microarray showed that BE treatment modulated the redox-related gene expression of the Bcl-2 family, such as Bid, Bad and Mc11, indicating that BE might decrease H9c2 cell apoptosis by modulating the mitochondrial redox status regulators. Altogether, these results suggest that BE may alleviate Dox-induced toxicity via anti-redox property and associated-gene modulation.

INTRODUCTION

Dox is one of the most effective anticancer drugs developed during recent decades because of its broad antitumor spectrum and high potency [1-3]. Similar to other anticancer agents, however, Dox may be toxic to healthy tissues as well as tumorous tissues. In addition to the common side effects of cancer chemotherapy, such as nausea, vomiting,

alopecia, mucosal ulceration, and hematopoietic suppression, Dox causes a unique type of cardiotoxicity that leads to chronic cardiomyopathy and drug-resistant congestive heart failure [4-6]. Although numerous mechanisms for this cardiotoxic effect, including DNA damage, disruption of Ca^{2+} homeostasis, cardiotoxic metabolites of Dox, impaired expression of cardiac proteins, and disruption of mitochondrial bioenergetics, have been proposed, the general consensus is that the redox cycling activity by Dox generates free radicals that mediate the various cytotoxic and cardiomyopathic effects [7-11]. Thus, redox navigation is one of the best strategies for reducing Dox-induced toxicity.

Redox is regarded as an important factor in the initiation and progression of many diseases, particularly ROS, which are by-products generated by cellular oxidative metabolism [12]. Therefore, measurements of redox status and process would be helpful in understanding the Dox-induced toxicity mechanism for several reasons.

Anthocyanins, one of the largest and most widespread group of pigments in fruits and vegetables, exert a multiplicity of biomedical functions that promote antioxidant status, healthy vision [13, 14], and urinary tract health [15, 16]. Anthocyanins have cardioprotective [17], antiangiogenic [18], anticarcinogenic [19-22], neuroprotective [23, 24], and antidiabetic properties [25, 26]. These biological activities are closely related to their potent redox properties. We previously reported that the cytoprotective effects of anthocyanins against Dox-induced toxicity in H9c2 cardiomyocytes could be explained, at least in part, by their ability to scavenge superoxide radicals generated by Dox [27].

Bilberry (*Vaccinium myrtillus* L.) is one of the richest anthocyanin sources, containing 300–600 mg/100 g fresh weight, and its anthocyanins consist of approximately 90% phenolic compounds [28, 29]. There is a growing global interest in bilberry because of its proposed health effects. Bilberry extracts are extensively used in dietary supplements and pharmaceutical products for improving vascular and vision disorders [30]. Many studies on bilberry have focused on anthocyanins because they are considered to be the most active components of bilberry [31-34].

In this study, we investigated the protective effects and the likely mechanism of BE against Dox-induced toxicity in H9c2 cardiomyocytes.

MATERIALS AND METHODS

Materials

BE, supplied by Nutrilite (Buena Park, CA, USA), was extracted using ethanol and was spray-dried and standardized to a minimum of 25% (w/w) anthocyanin. The anthocyanin profile and the contents of BE were analyzed using HPLC, as previously described [35]. BE contains five anthocyanidins (cyanidin, delphinidin, malvidin, peonidin and petunidin) glycosylated with three sugars, galactose, glucose and arabinose. Cyanidin (39%) and delphinidin glycosides (29%) are the major anthocyanins (data not shown). Dox was obtained from Ildong Pharmaceutical Co. (Seoul, Korea). Sulforhodamine B (SRB), butylated hydroxytoluene (BHT), 1-chloro-2,3-dinitrobenzene (CDNB), deoxyribose, dimethyl sulfoxide (DMSO), doxorubicin (Dox), ethylenediaminetetraacetic acid (EDTA), glutathione (GSH), reduced nicotinamide adenine dinucleotide (NADH), tetraethylbenzimidazolyl carbocyanine iodide (JC-1), sodium dodecyl sulfate (SDS), 2-thiobarbituric acid (TBA), and trichloroacetic acid (TCA) were purchased from Sigma Chemical Co. (St. Louis, MO, USA). The other chemicals used consisted of reagent grades.

Cell culture

H9c2 myocardiac cells (spontaneously immortalized ventricular myoblasts from a rat embryo) were purchased from American Type Culture Collection (Manassas, VA, USA). The

cells were cultured in complete Dulbecco's modified eagle's medium (DMEM) supplemented with 10% fetal bovine serum (FBS), 100 U/ml penicillin, and 0.1 mg/ml streptomycin at 37℃ in 5% CO_2. The cell culture medium and supplements were purchased from GibcoBRL (Grand Island, NY, USA). The medium was changed every 2 to 3 days.

Cell viability assay

Cell viability assays were performed using an SRB assay [36]. The cells were seeded into 96-well plates at 1.5×10^5 cells/ml and were incubated for 24 h before treatment. Thereafter, the cells were exposed to 1 µM Dox for 24 h and were incubated in fresh medium with BE at 0 to 100 µM for another 24 h. The cultures were stopped using 50% TCA solution and were subsequently incubated for 1 h at 4°C. The plates were washed with water five times and thoroughly dried. The dried plates were stained using 0.4% SRB solution in the dark for 30 min, and excess dye was washed out using 1% acetic acid. The unwashed dye was eluted with 10 mM Tris-buffer and was subsequently quantified spectrophotometrically at 550 nm using a microplate reader (Molecular Devices, Sunnyvale, CA, USA). Cytotoxicity was determined as the percentage of cell survival compared with that of Dox-treated control.

DNA fragmentation assay

Dox-induced apoptosis in H9c2 cells was confirmed by DNA fragmentation [37]. After a 24-h treatment using Dox and BE, the cells were washed twice with PBS and were collected by centrifugation at 3000 rpm for 5 min at 4°C. Genomic DNA was extracted using the QIAamp DNA extract kit (Qiagen, Hilden, Germany). The purified DNA was electrophoresed using 1.5% agarose gel, followed by ethidium bromide staining.

Caspase-3 activity assay

The caspase-3 activity [38] was determined using a commercially available kit (Sigma, St. Louis, MO, USA), which is based on the hydrolysis of the peptide substrate acetyl-Aso-GLu-Val-Asp p-nitroanilide (AC-DEVD-pNA) by caspase-3, resulting in the release of the p-nitroanilide (pNA) moiety. The H9c2 cells were lysed in lysis buffer (50 mM HEPES (pH 7.4), 5 mM CHAPS, 5 mM DTT and protease inhibitors), and 20 µg protein of each cell lysate was incubated in an assay buffer with 0.2 µmole of substrate for 6 h. The concentration of the pNA released from the substrate was measured spectrophotometrically at 405 nm and was calculated from a calibration curve prepared with defined pNA solutions. The caspase-3 activity was expressed as pmol pNA/min/mg protein.

MTP assay

MTP was measured using JC-1, which is a lipophilic, and cationic dye [39]. H9c2 cells cultured with Dox and BE on 24-well plates and 8-well chamber slides were loaded for 20 min at 37°C with 2 µg/ml of JC-1 in culture medium. The cells were washed twice using PBS, and the fluorescence level was immediately detected using a fluorometer (BMG LABTECH GmbH, Offenburg, Germany) and excitation of 485 nm and emission of 520 nm; the images were visualized using a microscope (Nikon, Tokyo, Japan). The ratio of measured intensity at both wavelengths is the indication for MTP.

Intracellular ROS measurement

Intracellular ROS induced by Dox was determined using 2' 7'-dichlorodihydrofluorescein diacetate (H_2DCFDA) (Molecular Probes, Eugene, OR, USA) [40]. The cells were incubated with 20 µM DCFH-DA at 37°C for 10 min. After DCFH-DA was removed, the cells were recorded. The DCFH-DA-loaded cells were placed in a fluorometer (BMG LABTECH GmbH) with excitation of 485 nm and

emission of 520 nm; the image was visualized using a microscope. The protein concentrations were determined using Bradford assays.

Lipid peroxidation assay

Lipid peroxide formation was analyzed by measuring the TBARS in the lysates as described by Jo et al., [41]. The 200 µl of cell lysates was transferred to test tubes, and 50 µl of BHT was added to prevent sporadic lipid peroxidation during heating. Subsequently, a solution of 1.5 ml of 0.5 M HCl, 1.5 ml of 20 mM TBA and distilled water was added. The reaction solution was well mixed and heated for 30 min in a boiling water bath. After cooling for 20 min, 2 ml of n-butanol was added. The solution was vigorously mixed and centrifuged at 3,000 rpm for 15 min. The TBARS levels were measured using a fluorometer and excitation and emission wavelengths of 515 nm and 555 nm, respectively (BMG LABTECH GmbH). The TBARS levels were calculated from a standard curve using 1,1,3,3-tetramethoxypropane and were normalized to the protein content.

GST activity assay

GST activity was spectrophotometrically assayed at 340 nm using the standard substrate CDNB and co-substrate GSH according to the method of Habig et al [42]. The increased rate of absorbance at 340 nm is directly proportional to GST activity. The activity was calculated using an extinction coefficient of 9.6 mM^{-1} cm^{-1} and was expressed as nmol of CDNB-GSH conjugate formed per min per mg protein.

GSH assay

The measurement of cellular GSH content was based on the GSH-recycling method [43]. The cell lysate was mixed using 5% sulfosalicylic acid and was centrifuged, and the supernatant was used for the assay. The assay mixture contained 0.4 mM NADPH; 1.64 units/mL GR was added into the sample or GSH standard and to each well. The mixture was incubated for 10 min at room temperature. After incubation with DTNB substrate solution for an additional 10 min, the absorbance at 405 nm was measured using a microplate reader (Molecular Devices, Sunnyvale, CA, USA).

Isolation of total RNA and microarray analysis

The total RNA from H9c2 cells was isolated using TRIzol (Invitrogen, Carlsbad, CA, USA) and was subsequently cleaned using the RNeasy Mini Kit (Qiagen GmbH, Hilden, Germany) [44]. Probe synthesis from total RNA (5 µg), hybridization, detection and scanning were performed according to the standard protocols (Affymetrix Inc., Santa Clara, CA, USA). cDNA was synthesized from total RNA using the one-cycle cDNA Synthesis Kit and T7-oligo (dT) primers. The double-stranded cDNA was used for in vitro transcription (IVT). cDNA was transcribed using the GeneChip IVT Labeling Kit (Affymetrix), and 10–15 µg of labeled cRNA was fragmented to form 35–200 bp fragments. After hybridization to the Rat 230 2.0 gene chips (Affymetrix) according to the Affymetrix standard protocol, the arrays were washed and stained using a streptavidin-phycoerythrin complex, and the intensities were determined using a GeneChip scanner 3000 (Affymetrix) and controlled using GCOS software 1.4 (Affymetrix). After data normalization, a DNA microarray data analysis was performed using GenPlexTM (Istech, Korea). The detectable expressed genes were defined using P-, M-, and A-calls according to the Affymetrix algorithm and the intensity of the genes. We selected only those genes with at least four P-calls. The cross comparisons of the control versus the treated data from each experiment were analyzed using the filtered probes. Only the genes that were significantly up or down regulated by at least two-fold compared with the control were judged to be valid and were identified as differentially expressed genes (DEGs).

Statistical analysis

The data are presented as the mean ± SEM values. The results were analyzed using Student's *t* test or one-way analysis of variance followed by Duncan's multiple range test using SPSS software (SPSS Inc., Chicago, IL, USA). $P < 0.05$ was considered to be statistically significant.

RESULTS

Effect of BE against Dox-induced cytotoxicity

To examine the protective effects of BE against Dox-induced myocardial toxicity, the cytotoxic effect of Dox was evaluated in cardiomyocytes. The half-maximal inhibitory concentration (IC_{50}) of Dox in H9c2 cells was determined to be approximately 1 μM; this concentration was chosen and used in additional experiments. The monomeric anthocyanin from bilberry extract (BA) was semi-purified using a solid-phase extraction and C18 cartridge (Sep-pak C18 plus, Waters Corporation, Milford, MA, USA) and was employed in the cytotoxicity assay. The 1-100 μg/ml of BA were equivalent to approximately 3-340 μg/ml of BE. The treatment using 5-50 μg/ml of BA (17-170 μg/ml of BE equivalent) significantly increased cell survival by 13% to 37% compared with the Dox-treated control in a dose-dependent manner. However, the protective effect decreased at a higher dose than 100 μg/ml of BA. To further evaluate whether BA modifies the chemosensitivity of Dox, the effect of BA on Dox-induced cytotoxicity was evaluated in MCF breast adenocarcinoma cells. BA had no effect on Dox-induced cytotoxicity, suggesting that BA does not interfere with the chemotherapeutic activity of Dox (Fig. 1).

Effect of BE against Dox-induced apoptosis

To determine the effects of BE on apoptosis induced by Dox in H9c2 cells, genomic DNA fragmentation by agarose gel electrophoresis was evaluated. As shown in Fig. 2A, DNA underwent internucleosomal cleavage after treatment with Dox, and BE treatment prevented DNA fragmentation. The activation of caspase-3, a key protein in the execution-phase of cell apoptosis, was investigated to confirm the protective effect of BE against Dox-induced apoptosis. H9c2 cells exposed to 1-μM Dox for 24 h showed a significant increase in the activity of caspase-3 by more than 10 times compared to that of the Dox-treated control, whereas the cells treated with Dox in combination with BE (50-100 μg/ml) showed a 27% to 68% decrease in the activity of caspase-3 in a dose-dependent manner (Fig. 2B).

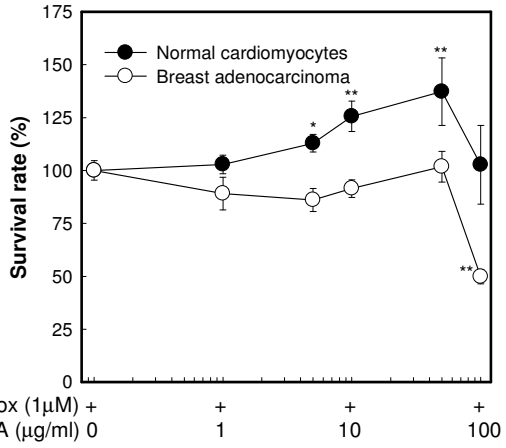

Fig.1: Effects of bilberry anthocyanin (BA) on the protective potential in normal cardiomyocytes (H9c2) and chemosensitivity in breast adenocarcinoma (MCF-7) in combination with Dox treatment. *BA was semi-purified from BE by a solid-phase extraction with C18 cartridge (Sep-pak C18 plus, Waters Corporation, Milford, MA, USA). The 1-100 μg/ml of BA were approximately equivalent to 3-340 μg/ml of BE. The values are presented as the mean ± SD. *p < 0.05, *p < 0.01, compared to the Dox-treated control.*

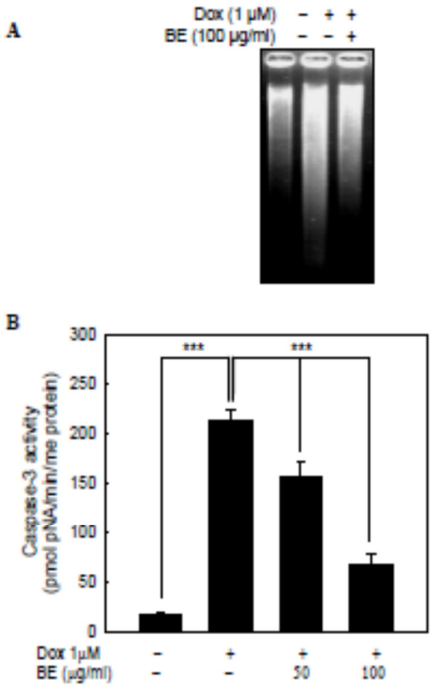

Fig.2: Inhibitory effect of BE against Dox-induced apoptosis in H9c2 cells.

*A: Effect of BE against dox-induced apototic DNA fragmentation. B: Effect of BE against Dox-induced caspase-3 activity. H9c2 cells were incubated 1 μM Dox and BE (50 and 100 μg/ml). After 24-h incubation, the cells were harvested and evaluated for DNA fragmentation and caspase-3 activity. The values are presented as the mean ± SD. ***p < 0.001, compared to the Dox-treated control.*

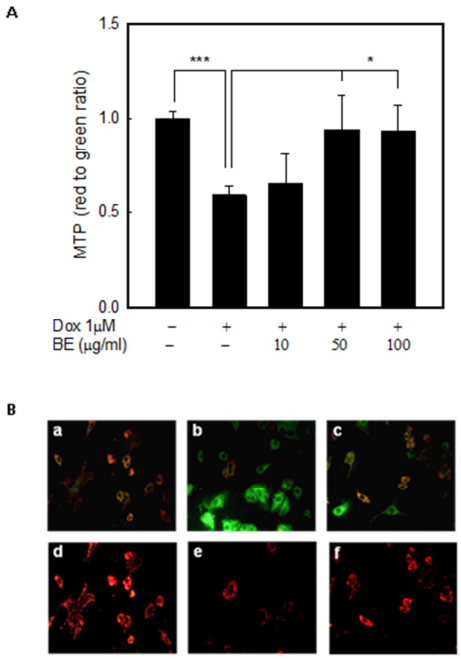

Fig.3: Change of MTP induced by Dox and BE in H9c2 cells.

*A: Fluorescence detection by fluorescence plate reader. B: Fluorescence images by microscope. a, d: normal control cells; b, e: cells exposed to Dox (1 μM); c, f: cells treated with Dox and BE. The values are presented as the mean ± SD. *p < 0.05, ***p < 0.01, compared to the Dox-treated control.*

Effect of BE against Dox-induced mitochondrial dysfunction

As shown in Fig. 3A, the red to green fluorescence ratio was decreased in the cells exposed to 1 μM of Dox, indicative of decreased mitochondrial membrane integrity; however, the cells treated with Dox and BE showed a significant increase in this ratio, which was nearly the same as the normal control. These results were further supported by the fluorescence imaging data, where the recovery of Dox-induced MTP loss by BE treatment could be observed (Fig. 3B).

Effect of BE against Dox-induced redox variation

Free radical may be one of the major causes of cytotoxic lesions. Therefore, we estimated free-radical generation using a TBARS assay. The effects of Dox and BE on the intracellular ROS formation are shown in Fig. 4. The cells exposed to Dox showed an increase in ROS levels, whereas these values were significantly reduced in H9c2 cells treated with BE for 1 h, in a dose-dependent manner, even at the lowest concentration. ROS initiate the autocatalytic chain of lipid peroxidation, resulting in the formation of a variety of toxic species and ultimately cell death. The MDA formation was analyzed by measuring the TBARS after a 24-h

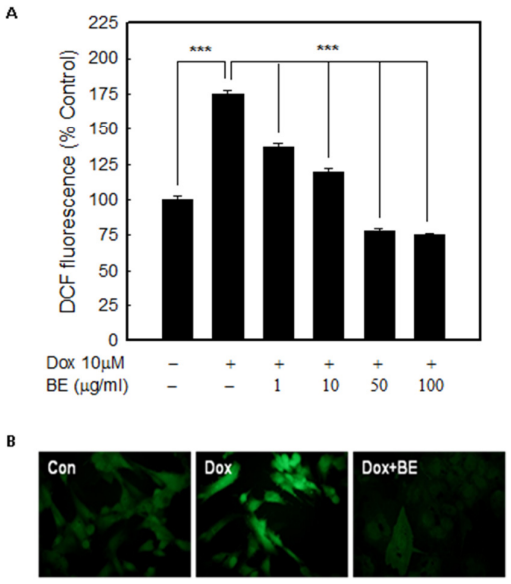

Fig.4: Scavenging effect of BE on Dox-induced intracellular ROS formation in H9c2 cells. *Intracellular ROS were determined by DCF assay. A: fluorescence detection using a microplate fluorescence reader; B: fluorescence images using a microscope. The values are presented as the mean ± SD. ***p < 0.001, compared to the Dox-treated control.*

exposure of H9c2 cells to 1 μM of Dox treatment. The result was significantly higher by approximately 38% compared to that of the Dox-untreated control. As shown in Fig. 5, the treatment using 50 μg/ml and 100 μg/ml of BE significantly reduced TBARS to a similar level as that of Dox-untreated control.

We analyzed the activity of cellular GST whose primary function is to catalyze the conjugation of electrophilic xenobiotics or their metabolites, including peroxides. The cellular GST activity is shown in Fig. 6A, illustrating that Dox treatment slightly decreased the GST activity. However, treatment with BE (50-100 μg/ml) increased the GST activity remarkably by 68% and 87%, respectively. Compared to that of the Dox-treated control, the activities of BE-treated cells were higher than those of Dox-untreated control. We evaluated the total GSH content in the same system. A significant decrease in GSH content was observed after Dox treatment. The Dox-treated cells had significantly lower levels of GSH than the untreated controls. Treatment with 50 μg/ml and 100 μg/ml of BE for 24 h significantly increased GSH levels up to 23% and 52% (Fig. 6B), which indicate that BE can protect cells against Dox-induced cytotoxicity through its antioxidant effects.

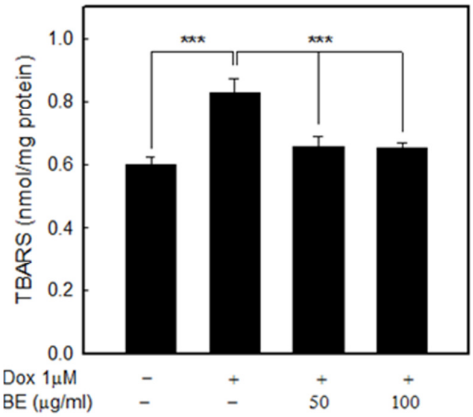

Fig.5: Effect of BE on Dox-induced lipid peroxidation in H9c2 cells. *After a 24-h exposure to 1 μM Dox and BE (50 and 100 μg/ml), lipid peroxidation was assessed using the TBARS assay. The values are presented as the mean ± SD. ***p < 0.001, compared to the Dox-treated control.*

Altered gene expression by Dox and BE treatments in H9c2 cells

The numeric distribution of total genes and the DEG treated using 1 μM of Dox and BE in H9c2 cells is demonstrated. Dox and BE treatments in H9c2 cells caused significant changes in gene expression or redox response by another classification as shown in Table 1. Among DEGs related to apoptosis, Bid, Bad, Bak1 and Mc11 belong to the Bcl-2 family. Proapoptotic members, Bid and Bad were upregulated by Dox treatment but downregulated by BE treatment. Moreover, Nol3, Bcap29 and Bcap31 expressions were altered. Dox upregulated the levels of antioxidant enzymes, GST and GPx, but downregulated by BE. In contrast, Gsr was

downregulated by Dox but upregulated by BE. Several heat shock proteins (HSP) were modulated by Dox and BE.

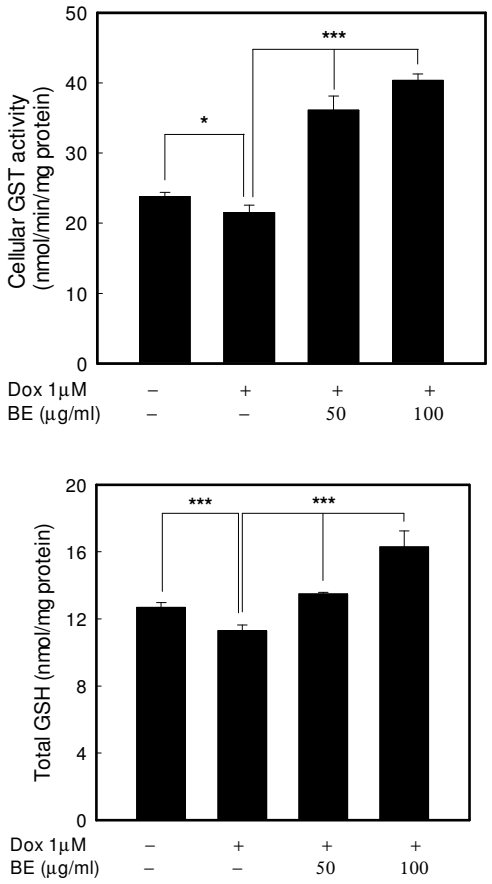

Fig.6: Effects of BE on Dox-induced GST activity and GSH level in H9c2 cells. A: After a 24-h exposure to 1 μM Dox and BE (50 and 100 μg/ml), GST activities were subsequently assessed using CDNB. B: GSH level was determined by the GSH-recycling method using DTNB. The values are presented as the mean ± SD. *$p < 0.05$, ***$p < 0.001$, compared to the Dox-treated control.

DISCUSSION

Our results demonstrated the effect of BE against Dox-induced cardiotoxicity. Dox treatment caused cytotoxicity, apoptosis, mitochondrial dysfunction, intracellular ROS generation and lipid peroxidation in H9c2 cardiomyocytes. The addition of anthocyanin-rich BE to H9c2 cells provided significant cytoprotection against Dox-induced cardiotoxicity without interfering with the chemosensitivity of Dox, and it also provided reduction against Dox-induced apoptosis, mitochondrial dysfunction, lipid peroxidation and intracellular ROS generation, as well as a significant induction of GSH and GST activity in H9c2 cardiomyocytes.

Although Dox is an anthracycline antibiotic and is one of the most effective and widely used anticancer medications, the clinical use of Dox has been limited due to the development of life-threatening cardiomyopathy and congestive heart failure [4, 5, 45]. Many studies have demonstrated that the apoptosis of cardiomyocytes via the mitochondrial pathway, which is characterized by the disruption of MTP, cytochrome c release, caspase activation, and genomic DNA cleavage, contributes to the development of myocardial dysfunction in heart failure. ROS as a by-product of Dox metabolism is considered to be the primary mechanism of Dox-induced cardiotoxicity. Dox is accumulated within the mitochondrion, and then NADH dehydrogenase (complex 1) in mitochondria as the reductive enzyme results in producing the majority of ROS from the Dox redox cycling in cardiomyocytes [46-48]. MTP is essential for the maintenance of mitochondrial function. It has been reported that the superoxide radical ($\dot{O}_2$) is reduced at reoxygenation by opening the mitochondrial K_{ATP} channel [49]. MTP is injured because of the opening of permeability transition pores at an early stage of apoptosis [50]. A loss of MTP in myocytes is accompanied by the release of cytochrome c from mitochondria into the cytosol, where it triggers the formation of the apoptosome, composed of apoptotic protease activating factor-1 (Apaf-1), dATP and cytochrome c.

Table 1: DEGs related to apoptosis or redox response

Acc. no.	Symbol	Gene name	Fold change	
			Dox /Con	Dox+BE /Dox
Apoptosis-related genes				
XM_231137	*Abl1*	c-abl oncogene 1, non-receptor tyrosine kinase	-3.26	1.87
XM_240178	*Acin1*	apoptotic chromatin condensation inducer 1	-1.57	1.55
XM_001071044	*Api5*	apoptosis inhibitor 5	-1.62	1.89
NM_032072	*Nae1*	NEDD8 activating enzyme E1 subunit 1	-2.47	2.08
NM_053812	*Bak1*	BCL2-antagonist/killer 1	-2.87	2.35
NM_012513	*Bdnf*	Brain-derived neurotrophic factor	-1.80	1.96
XM_001055775	*Bnip2*	BCL2/adenovirus E1B interacting protein 2	-1.58	1.53
NM_001007798	*Btk*	Bruton agammaglobulinemia tyrosine kinase	-1.67	1.81
NM_024125	*Cebpb*	CCAAT/enhancer-binding protein (C/EBP), beta	-2.12	4.06
NM_057138	*Cflar*	CASP8 and FADD-like apoptosis regulator	-1.88	1.53
XM_235061	*Cradd*	CASP2 and RIPK1 domain containing adaptor with death domain	-1.64	1.77
XM_001069456	*Cul1*	cullin 1	-2.18	2.51
XM_217454	*Cul3*	cullin 3	-2.63	2.40
NM_130406	*Faf1*	Fas (TNFRSF6) associated factor 1	-2.59	1.87
XM_345868	*Hdac7*	histone deacetylase 7	-2.57	1.68
XM_001071106	*Hip1*	huntingtin interacting protein 1	-3.08	1.83
NM_052807	*Igf1r*	insulin-like growth factor 1 receptor	-3.77	2.07
XM_001060304	*Hspc159*	galectin-related protein	-2.42	1.62
NM_021846	*Mcl1*	myeloid cell leukemia sequence 1	-1.59	1.65
XM_219708	*Ndnl2*	necdin-like 2	-1.52	1.77
NM_053516	*Nol3*	nucleolar protein 3 (apoptosis repressor with CARD domain)	-1.59	1.64
NM_033485	*Pawr*	PRKC, apoptosis, WT1, regulator	-1.72	2.36
XM_214911	*Pdcd5*	programmed cell death 5	-1.80	1.55
XM_217732	*Pdcd6*	programmed cell death 6	-1.71	1.91
XM_001054328	*Rgd1564174*	similar to novel protein similar to Tensin Tns	-2.62	2.06
NM_012747	*Stat3*	signal transducer and activator of transcription 3	-1.60	1.61
XM_001069237	*Tec*	tec protein-tyrosine kinase	-2.22	1.50
XM_214962	*Tm2d3*	Trans membrane 2 domain containing 3	-2.34	2.52
NM_013091	*Tnfrsf1a*	tumor necrosis factor receptor superfamily, member 1a	-1.95	1.96
NM_022207	*Unc5b*	unc-5 homolog B (*C. elegans*)	-2.18	1.56
NM_199407	*Unc5c*	unc-5 homolog C (*C. elegans*)	-1.64	1.83
XM_001080939	*Wdr22*	WD repeat domain 22	-1.77	1.62
NM_022698	*Bad*	Bcl2-antagonist of cell death	2.24	-1.66
NM_001006980	*Bcap29*	B-cell receptor-associated protein 29	1.55	-2.43
NM_001004224	*Bcap31*	B-cell receptor-associated protein 31	2.47	-1.64
NM_022684	*Bid*	BH3 interacting domain death agonist	2.04	-1.57
NM_012524	*Cebpa*	CCAAT/enhancer-binding protein (C/EBP), alpha	2.15	-1.66
NM_178334	*Egln1*	EGL nine homolog 1 (*C. elegans*)	1.57	-1.79
NM_199114	*Fgfrl1*	fibroblast growth factor receptor-like 1	2.87	-3.98

XM_001076962	*Fis1*	fission 1 (mitochondrial outer membrane) homolog (*S. cerevisiae*)	1.96	-2.38
NM_024127	*Gadd45a*	growth arrest and DNA-damage-inducible, alpha	1.76	2.56
NM_012589	*Il6*	interleukin 6	1.61	2.04
NM_031832	*Lgals3*	lectin, galactoside-binding, soluble, 3	2.18	2.60
XM_001054123	*Mycl*	v-myc myelocytomatosis viral oncogene homolog, lung carcinoma derived (avian)	6.53	-4.46
NM_053373	*Pglyrp1*	peptidoglycan recognition protein 1	1.84	2.51
NM_054001	*Scarb2*	scavenger receptor class B, member 2	1.90	-2.10
XM_001067297	*Relt*	RELT tumor necrosis factor receptor	2.20	-2.00
Stress response-related genes				
NM_001007680	*Abhd6*	abhydrolase domain containing 6	-2.13	1.51
NM_001007798	*Btk*	Bruton agammaglobulinemia tyrosine kinase.	-1.67	1.81
NM_032079	*Dnaja2*	DnaJ (Hsp40) homolog, subfamily A, member 2	-2.29	2.72
XM_223030	*Dusp10*	dual specificity phosphatase 10	-1.51	2.12
NM_053906	*Gsr*	glutathione reductase	-2.19	2.53
NM_013083	*Hspa5*	heat shock protein 5	-1.78	2.19
XM_214583	*Hspa9*	heat shock protein 9	-1.69	2.46
NM_022229	*Hspd1*	heat shock protein 1 (chaperonin)	-1.92	1.83
NM_212505	*Ier3*	immediate early response 3	-2.21	2.46
XM_224824	*Rgd1561618*	similar to Chain A, T13s mutant of bovine 70-kilodalton heat shock protein	-2.28	2.47
XR_008535	*Hspa8*	heat shock 70 kDa protein 8	-2.32	2.56
NM_134410	*Mosc2*	MOCO sulfurase C-terminal domain containing 2	-1.56	1.50
XM_214157	*Parp2*	poly (ADP-ribose) polymerase 2	-3.28	2.16
NM_053999	*Ppp2r2a*	protein phosphatase 2 (formerly 2A), regulatory subunit B, alpha isoform	-1.93	2.17
NM_013173	*Slc11a2*	solute carrier family 11 (proton-coupled divalent metal ion transporters), member 2	-2.76	1.90
NM_001034090	*Ephx1*	epoxide hydrolase 1, microsomal	2.32	2.09
NM_030826	*Gpx1*	glutathione peroxidase 1	1.82	-1.58
XM_001060175	*Gpx7*	glutathione peroxidase 7	2.11	-2.87
NM_017014	*Gstm1*	glutathione S-transferase, mu 1	1.81	-2.00
NM_177426	*Gstm2*	glutathione S-transferase, mu 2	2.12	-2.11
NM_172038	*Gstm5*	glutathione S-transferase, mu 5	2.89	-3.44
NM_012796	*Gstt2*	glutathione S-transferase, theta 2	2.42	-1.50
NM_033349	*Hagh*	hydroxyacyl glutathione hydrolase	2.58	-1.74
NM_021863	*Hspa2*	heat shock protein 2	2.19	-2.47
NM_138887	*Hspb6*	heat shock protein, alpha-crystalline-related, B6	1.58	-2.07
NM_019328	*Nr4a2*	nuclear receptor subfamily 4, group A, member 2	2.39	-2.81
NM_031628	*Nr4a3*	nuclear receptor subfamily 4, group A, member 3	2.72	-2.19
NM_001013082	*Pon2*	paraoxonase 2	1.77	-2.22
NM_022627	*Prkab2*	protein kinase, AMP-activated, beta 2 non-catalytic subunit	1.55	-1.97
NM_012808	*Tst*	thiosulfate sulfotransferase, mitochondrial	1.87	-1.80
NM_053800	*Txn1*	thioredoxin 1	1.54	-1.53

At present, the only known function of the apoptosome is the recruitment and activation of caspase-9. The caspase-9/apoptosome complex targets activated caspase-3. Therefore, this process is suggested to be irreversible in the apoptotic signaling cascade [51, 52].

In the present study, BE was observed to reduce intracellular ROS, restore MTP, inhibit caspase-3 activity, and eventually reduce apoptosis and cell death. It was elucidated that anthocyanins could directly scavenge $\dot{O}_2$, H_2O_2, peroxynitrite and nitric oxides more effectively than Vt C. It has also been reported that berry phenolics and bilberry anthocyanins might be capable of scavenging free radicals [53, 54]. Other flavonoids, monohydroxy methyl fructoside, naringenin and proanthocyanidin have been evaluated in various experimental models for their potentials to reduce Dox-induced cardiotoxicity, related to their antioxidant and iron chelating activities [55-57]. In particular, the scavenging of superoxide against Dox-induced toxicity in H9c2 cells is important because this radical is ubiquitous in aerobic cells and, despite its mild reactivity, is a potential precursor of the aggressive hydroxyl radical in the Fenton and Haber-Weiss reactions [27, 35, 58].

Recently, flavonoids can function as stress protectants in cells by scavenging ROS. Their radical scavenging activity depends on structure-activity relationships, as suggested by Rice-Evans et al [59]. Anthocyanidins and their glycosides (anthocyanins) are equipotent to quercetin and catechin gallates, provided that a catechol structure is present in ring B. More specifically, the major determinants of the radical-scavenging capability of anthocyanins are as follows: (i) the presence of a catechol group in ring, which has better electron-donating properties; (ii) a 2, 3 double bond conjugated with the 4-oxo group, which is responsible for electron delocalization; and (iii) a formation of aroxyl radical [60].

Moreover, the direct scavenging activity of BE significantly induced the activities of cellular GSTs (Fig. 6A). GSTs belong to a large and diverse group of phase II biotransformation enzymes that function in the detoxification of xenobiotics and endogenous toxicants. Several GST isoenzymes, especially alpha class GSTs, can efficiently reduce fatty acid hydroperoxides as well as phospholipid hydroperoxides and can disrupt the autocatalytic chain of lipid peroxidation chain reactions [61]. Furthermore, GST alpha 1 and 2 can use member phospholipid hydroperoxides as substrates in situ and can protect cell membranes at the sites of damage [62, 63]. Choi et al have previously reported that induction of GST in H9c2 cells may serve as protection against Dox-induced cytotoxicity in H9c2 cells [64]. Additionally, Milbury et al have demonstrated that bilberry anthocyanin upregulated the oxidative stress defense enzymes, such as heme oxygenase-1 and GST-pi, in retinal pigment epithelial cells [33]. In this regard, these results demonstrated that the induction of GSTs by BE may contribute, at least in part, to the increased resistance of BE-treated cells to the Dox-induced cytotoxicity. Additionally, the depletion of GSH by Dox was recovered nearly to the normal control level by BE treatment in a dose-dependent manner (Fig. 6B). Evidence has suggested that GSH depletion markedly increases Dox-induced cytotoxicity [65, 66]. The lowered GSH levels observed in our study might reflect the increased consumption of GSH in the detoxification of ROS generated by Dox. The increase in GSH content by BE treatment might help to promote the nonenzymatic scavenging ROS and the enzymatic detoxification of organic peroxides and, thus, protect against Dox-induced cardiotoxicity.

Among DEGs related to apotosis, Bid, Bad Bak1 and Mc11 belong to the Bcl-2 family, which directly modulate mitochondrial membrane permeability and thereby regulate the release of apoptogenic factors from the intermembrane space into the cytoplasm [67]. Nol3, Bcap29 and Bcap31 were altered by Dox and BE was related to caspase-8 activation. Thus, BE treatment might reduce mitochondrial apoptosis via the modulation of gene expression in the Bcl-2 family. The expression pattern of GSTs by Dox

and BE showed an opposite result with enzyme activity.

CONCLUSION

Our results demonstrated that BE may have a protective potential against the Dox-induced cardiotoxicity in H9c2 cells. The protective actions of BE were highly related with redox properties, especially the scavenging redox cycling of Dox and restoring GSH.

CONFLICT OF INTEREST STATEMENT

The authors declare that they have no potential conflicts of interest with anyone at their institute or with any other party regarding the publication of the data in the present study.

ACKNOWLEDGEMENTS

This work was supported, in part, by the Bio-Synergy Research Project (NRF-2013 M3A9C4078156) of the Ministry of Science, ICT and Future Planning through the National Research Foundation, by the Chung-Ang University Excellent Student Scholarship.

REFERENCES

1. Minotti G, Menna P, Salvatorelli E et al. Anthracyclines: molecular advances and pharmacologic developments in antitumor activity and cardiotoxicity. Pharmacol Rev 2004;56:185-229.
2. Weiss RB. The anthracyclines: will we ever find a better doxorubicin? Semin Oncol 1992;19:670-686.
3. Blum RH, Carter SK. Adriamycin. A new anticancer drug with significant clinical activity. Ann Intern Med 1974;80:249-259.
4. Von Hoff DD, Layard MW, Basa P, et al. Risk factors for doxorubicin-induced congestive heart failure. Ann Intern Med 1979;91:710-717.
5. Doroshow JH. Doxorubicin-induced cardiac toxicity. N Engl J Med 1991;324:843-845.
6. Singal PK, Iliskovic N. Doxorubicin-induced cardiomyopathy. N Engl J Med 1998; 339: 900-905.
7. Minotti G, Cairo G, Monti E. Role of iron in anthracycline cardiotoxicity: new tunes for an old song? FASEB J 1999;13:199-212.
8. Goodman J, Hochstein P. Generation of free radicals and lipid peroxidation by redox cycling of adriamycin and daunomycin. Biochem Biophys Res Commun 1977;77:797-803.
9. Gille L, Nohl H. Analyses of the molecular mechanism of adriamycin-induced cardiotoxicity. Free Radic Biol Med 1997;23:775-782.
10. Simunek T, Sterba M, Popelova O et al. Anthracycline-induced cardiotoxicity: overview of studies examining the roles of oxidative stress and free cellular iron. Pharmacol Rep 2009;61:154-171.
11. Granados-Principal S, Quiles JL, Ramirez-Tortosa CL, et al. New advances in molecular mechanisms and the prevention of adriamycin toxicity by antioxidant nutrients. Food Chem Toxicol 2010;48:1425-1438.
12. Han JY, Hong JT, Oh KW. In vivo electron spin resonance: An effective new tool for reactive oxygen species/reactive nitrogen species measurement. Arch Pharm Res 2010; 33: 1293-1299.
13. Matsumoto H, Nakamura Y, Tachibanaki S et al. Stimulatory effect of cyanidin 3-glycosides on the regeneration of rhodopsin. J Agric Food Chem 2003;51:3560-3563.
14. Jang YP, Zhou J, Nakanishi K et al. Anthocyanins protect against A2E photooxidation and membrane permeabilization in retinal pigment epithelial cells. Photochem Photobiol 2005;81:529-536.
15. Dearing MD, Appel HM, Schultz JC. Why do cranberries reduce incidence of urinary tract infections? J Ethnopharmacol 2002;80:211.
16. Ohnishi R, Ito H, Kasajima N et al. Urinary excretion of anthocyanins in humans after cranberry juice ingestion. Biosci Biotechnol Biochem 2006;70:1681-1687.

17. Mullen W, McGinn J, Lean ME et al. Ellagitannins, flavonoids, and other phenolics in red raspberries and their contribution to antioxidant capacity and vasorelaxation properties. J Agric Food Chem 2002;50:5191-5196.
18. Bagchi D, Sen CK, Bagchi M et al. Anti-angiogenic, antioxidant, and anti-carcinogenic properties of a novel anthocyanin-rich berry extract formula. Biochemistry (Mosc) 2004;69:75-80, 71 p preceding 75.
19. Zhao C, Giusti MM, Malik M et al. Effects of commercial anthocyanin-rich extracts on colonic cancer and nontumorigenic colonic cell growth. J Agric Food Chem 2004; 52: 6122-6128.
20. Hou DX. Potential mechanisms of cancer chemoprevention by anthocyanins. Curr Mol Med 2003;3:149-159.
21. Katsube N, Iwashita K, Tsushida T et al. Induction of apoptosis in cancer cells by Bilberry (Vaccinium myrtillus) and the anthocyanins. J Agric Food Chem 2003; 51:68-75.
22. Meiers S, Kemeny M, Weyand U et al. The anthocyanidins cyanidin and delphinidin are potent inhibitors of the epidermal growth-factor receptor. J Agric Food Chem 2001; 49: 958-962.
23. Youdim KA, Shukitt-Hale B, MacKinnon S et al. Polyphenolics enhance red blood cell resistance to oxidative stress: in vitro and in vivo. Biochim Biophys Acta 2000;1523:117-122.
24. Galli RL, Shukitt-Hale B, Youdim KA et al. Fruit polyphenolics and brain aging: nutritional interventions targeting age-related neuronal and behavioral deficits. Ann N Y Acad Sci 2002;959:128-132.
25. Matsui T, Ogunwande IA, Abesundara KJ et al. Anti-hyperglycemic Potential of Natural Products. Mini Rev Med Chem 2006;6:349-356.
26. Cignarella A, Nastasi M, Cavalli E et al. Novel lipid-lowering properties of Vaccinium myrtillus L. leaves, a traditional antidiabetic treatment, in several models of rat dyslipidaemia: a comparison with ciprofibrate. Thromb Res 1996;84:311-322.
27. Choi EH, Chang HJ, Cho JY et al. Cytoprotective effect of anthocyanins against doxorubicin-induced toxicity in H9c2 cardiomyocytes in relation to their antioxidant activities. Food Chem Toxicol 2007;45:1873-1881.
28. Latti AK, Riihinen KR, Kainulainen PS. Analysis of anthocyanin variation in wild populations of bilberry (Vaccinium myrtillus L.) in Finland. J Agric Food Chem 2008;56:190-196.
29. Kahkonen MP, Hopia AI, Vuorela HJ et al. Antioxidant activity of plant extracts containing phenolic compounds. J Agric Food Chem 1999;47:3954-3962.
30. European Scientific Cooperative on Phytotherapy (ESCOP) Monographs 345–350.
31. Bao L, Yao XS, He RR et al. Protective effects of Guangdong Liangcha grandes on restraint stress-induced liver damage in mice. Zhongguo Zhong Yao Za Zhi 2008;33:664-669.
32. Heinonen M. Antioxidant activity and antimicrobial effect of berry phenolics--a Finnish perspective. Mol Nutr Food Res 2007;51:684-691.
33. Milbury PE, Graf B, Curran-Celentano JM et al. Bilberry (Vaccinium myrtillus) antho-cyanins modulate heme oxygenase-1 and glutathione S-transferase-pi expression in ARPE-19 cells. Invest Ophthalmol Vis Sci 2007;48:2343-2349.
34. Ichiyanagi T, Shida Y, Rahman MM et al. Bioavailability and tissue distribution of anthocyanins in bilberry (Vaccinium myrtillus L.) extract in rats. J Agric Food Chem 2006; 54:6578-6587.
35. Choi EH, Ok HE, Yoon Y et al. Protective effect of anthocyanin-rich extract from bilberry (Vaccinium myrtillus L.) against myelotoxicity induced by 5-fluorouracil.

Biofactors 2007;29:55-65.
36. Skehan P, Storeng R, Scudiero D et al. New colorimetric cytotoxicity assay for anticancer-drug screening. J Natl Cancer Inst 1990;82:1107-1112.
37. Ioannou YA, Chen FW. Quantitation of DNA fragmentation in apoptosis. Nucleic Acids Res 1996;24:992-993.
38. Wang GW, Klein JB, Kang YJ. Metallothionein inhibits doxorubicin-induced mitochondrial cytochrome c release and caspase-3 activation in cardiomyocytes. J Pharmacol Exp Ther 2001;298:461-468.
39. Nuydens R, Novalbos J, Dispersyn G et al. A rapid method for the evaluation of compounds with mitochondria-protective properties. J Neurosci Methods 1999;92:153-159.
40. Wang H, Joseph JA. Quantifying cellular oxidative stress by dichlorofluorescein assay using microplate reader. Free Radic Biol Med 1999;27:612-616.
41. Jo C, Ahn DU. Fluorometric analysis of 2-thiobarbituric acid reactive substances in turkey. Poult Sci 1998;77:475-480.
42. Habig WH, Pabst MJ, Jakoby WB. Glutathione S-transferases. The first enzymatic step in mercapturic acid formation. J Biol Chem 1974;249:7130-7139.
43. Shaik IH, Mehvar R. Rapid determination of reduced and oxidized glutathione levels using a new thiol-masking reagent and the enzymatic recycling method: application to the rat liver and bile samples. Analytical and bioanalytical chemistry 2006;385:105-113.
44. Kruhoffer M, Dyrskjot L, Voss T et al. Isolation of microarray-grade total RNA, microRNA, and DNA from a single PAXgene blood RNA tube. J Mol Diagn 2007;9:452-458.
45. Singal PK, Li T, Kumar D et al. Adriamycin-induced heart failure: mechanism and modulation. Mol Cell Biochem 2000;207:77-86.
46. Bachur NR, Gee MV, Friedman RD. Nuclear catalyzed antibiotic free radical formation. Cancer Res 1982;42:1078-1081.
47. Doroshow JH, Davies KJ. Redox cycling of anthracyclines by cardiac mitochondria. II. Formation of superoxide anion, hydrogen peroxide, and hydroxyl radical. J Biol Chem 1986;261:3068-3074.
48. Yee SB, Pritsos CA. Comparison of oxygen radical generation from the reductive activation of doxorubicin, streptonigrin, and menadione by xanthine oxidase and xanthine dehydrogenase. Arch Biochem Biophys 1997;347:235-241.
49. Hoek T, Becker L, Z. S et al. Preconditioning in cardiomyocytes protects by attenuating oxidant stress at reperfusion. Am Heart Assoc 2000:541-548.
50. Zamzami N, Susin SA, Marchetti P et al. Mitochondrial control of nuclear apoptosis. J Exp Med 1996;183:1533-1544.
51. Cain K, Bratton SB, Cohen GM. The Apaf-1 apoptosome: a large caspase-activating complex. Biochimie 2002;84:203-214.
52. Hu Y, Ding L, Spencer DM et al. WD-40 repeat region regulates Apaf-1 self-association and procaspase-9 activation. J Biol Chem 1998;273:33489-33494.
53. Ichiyanagi T, Hatano Y, Matsugo S et al. Simultaneous comparison of relative reactivities of twelve major anthocyanins in bilberry towards reactive nitrogen species. Chem Pharm Bull (Tokyo) 2004;52:1312-1315.
54. Zheng W, Wang SY. Oxygen radical absorbing capacity of phenolics in blueberries, cranberries, chokeberries, and lingonberries. J Agric Food Chem 2003;51:502-509.
55. Bast A, Kaiserova H, den Hartog GJ et al. Protectors against doxorubicin-induced cardiotoxicity: flavonoids. Cell Biol Toxicol 2007;23:39-47.
56. Han X, Ren D, Fan P et al. Protective effects of naringenin-7-O-glucoside on doxorubicin-induced apoptosis in H9C2 cells. Eur J Pharmacol 2008;581:47-53.
57. Zhang XY, Li WG, Wu YJ et al. Proantho-

cyanidin from grape seeds enhances doxorubicin-induced antitumor effect and reverses drug resistance in doxorubicin-resistant K562/DOX cells. Can J Physiol Pharmacol 2005;83:309-318.
58. Cao G, Sofic E, Prior RL. Antioxidant and prooxidant behavior of flavonoids: structure-activity relationships. Free Radic Biol Med 1997;22:749-760.
59. Rice-Evans CA, Miller NJ, Paganga G. Structure-antioxidant activity relationships of flavonoids and phenolic acids. Free Radic Biol Med 1996;20:933-956.
60. Han JY, Ahn SY, Kim CS, et al. Protection of apigenin against kainate-induced excito-toxicity by anti-oxidative effects. Biol Pharm Bull 2012;35:1440-1446.
61. Hayes JD, Flanagan JU, Jowsey IR. Gluta-thione transferases. Annu Rev Pharmacol Toxicol 2005;45:51-88.
62. Yang Y, Cheng JZ, Singhal SS, et al. Role of glutathione S-transferases in protection against lipid peroxidation. Overexpression of hGSTA2-2 in K562 cells protects against hydrogen peroxide-induced apoptosis and inhibits JNK and caspase 3 activation. J Biol Chem 2001;276:19220-19230.
63. Sharma R, Yang Y, Sharma A et al. Antioxidant role of glutathione S-transfe-rases: protection against oxidant toxicity and regulation of stress-mediated apoptosis. Antioxid Redox Signal 2004;6:289-300.
64. Choi EH, Lee N, Kim HJ et al. Schisandra fructus extract ameliorates doxorubicin-induce cytotoxicity in cardiomyocytes: altered gene expression for detoxification enzymes. Genes & nutrition 2008;2:337-345.
65. Mohamed HE, El-Swefy SE, Hagar HH. The protective effect of glutathione administration on adriamycin-induced acute cardiac toxicity in rats. Pharmacol Res 2000;42:115-121.
66. Yin X, Wu H, Chen Y et al. Induction of antioxidants by adriamycin in mouse heart. Biochem Pharmacol 1998;56:87-93.
67. Tsujimoto Y. Cell death regulation by the Bcl-2 protein family in the mitochondria. J Cell Physiol 2003;195:158-167.

Cite this article as:
Eun Hye Choi, Jin-Yi Han, Ju Hee Kang, Mi Kyung Kim, Hyang Sook Chun. Alleviation of Doxorubicin-Induced Cardiocytotoxicity by Anthocyanin-Rich Bilberry (Vaccinium myrtillus L.) in H9c2 Cells by Antioxidative Effects. J Pharm Chem Biol Sci 2015; 3(2): 247-261